the plant journal

SEB SOCIETY FOR EXPERIMENTAL BIOLOGY

The Plant Journal (2024) **118,** 1102–1118 doi: 10.1111/tpj.16659

Cytonuclear interplay in auto- and allopolyploids: a multifaceted perspective from the *Festuca-Lolium* complex

Mehrdad Shahbazi[1,2], Joanna Majka[1,3], Denisa Kubíková[1], Zbigniew Zwierzykowski[3], Marek Glombik[1,4], Jonathan F. Wendel[5], Joel Sharbrough[6], Stephan Hartmann[7], Marek Szecówka[1], Jaroslav Doležel[1], Jan Bartoš[1], David Kopecký[1,*] and Jana Kneřová[1,*]

[1]*Institute of Experimental Botany of the Czech Academy of Sciences, Centre of Plant Structural and Functional Genomics, Šlechtitelů 31, 77900 Olomouc, Czech Republic,*

[2]*National Centre for Biomolecular Research, Faculty of Science, Masaryk University, Kotlářská 2, 61137 Brno, Czech Republic,*

[3]*Department of Environmental Stress Biology, Institute of Plant Genetics, Polish Academy of Sciences, Strzeszyńska 34, 60-479 Poznań, Poland,*

[4]*Department of Crop Genetics, John Innes Centre, Norwich NR4 7UH, UK,*

[5]*Department of Ecology, Evolution, and Organismal Biology, Iowa State University, Ames IA 50011 Iowa, USA,*

[6]*New Mexico Institute of Mining and Technology, Biology Department, Socorro, New Mexico 87801, USA, and*

[7]*Bavarian State Research Center for Agriculture (LfL), Institute for Crop Science and Plant Breeding, Am Gereuth 4, 85354 Freising, Germany*

Received 1 November 2023; revised 15 December 2023; accepted 22 January 2024; published online 7 February 2024.
*For correspondence (e-mail kopecky@ueb.cas.cz, szecowkaj@ueb.cas.cz).

SUMMARY

Restoring cytonuclear stoichiometry is necessary after whole-genome duplication (WGD) and interspecific/intergeneric hybridization in plants. We investigated this phenomenon in auto- and allopolyploids of the *Festuca-Lolium* complex providing insights into the mechanisms governing cytonuclear interactions in early polyploid and hybrid generations. Our study examined the main processes potentially involved in restoring the cytonuclear balance after WGD comparing diploids and new and well-established autopolyploids. We uncovered that both the number of chloroplasts and the number of chloroplast genome copies were significantly higher in the newly established autopolyploids and grew further in more established autopolyploids. The increase in the copy number of the chloroplast genome exceeded the rise in the number of chloroplasts and fully compensated for the doubling of the nuclear genome. In addition, changes in nuclear and organelle gene expression were insignificant. Allopolyploid *Festuca* × *Lolium* hybrids displayed potential structural conflicts in parental protein variants within the cytonuclear complexes. While biased maternal allele expression has been observed in numerous hybrids, our results suggest that its role in cytonuclear stabilization in the *Festuca* × *Lolium* hybrids is limited. This study provides insights into the restoration of the cytonuclear stoichiometry, yet it emphasizes the need for future research to explore post-transcriptional regulation and its impact on cytonuclear gene expression stoichiometry. Our findings may enhance the understanding of polyploid plant evolution, with broader implications for the study of cytonuclear interactions in diverse biological contexts.

Keywords: allopolyploidy, autopolyploidy, chloroplast, cytonuclear interactions, *Festuca pratensis* Huds., gene expression, *Lolium multiflorum* lam., organelle DNA, protein modeling, whole genome duplication.

INTRODUCTION

Interspecific hybridization and polyploidization are important processes driving plant evolution. Angiosperms have experienced numerous whole genome duplication events (WGD) during their history, contributing to their diversification (Bomblies, 2020; Fox et al., 2020; Jiao et al., 2011; Soltis & Soltis, 2009, 2016; Van de Peer et al., 2017, 2021). Polyploids are broadly classified as autopolyploids, arising from WGD within a species, and allopolyploids, resulting from hybridization of distinct species, followed or preceded by WGD. Interspecific hybridization and polyploidization have played significant roles in the origin of major crops

such as wheat, oilseed rape, banana, and cotton (Renny-Byfield & Wendel, 2014; Salman-Minkov et al., 2016; Wendel, 2015).

The prevalence of polyploidy in angiosperms suggests that at least under some circumstances it generates selective advantages. This observation notwithstanding, newly formed auto- and allopolyploids face survival challenges due to genic incompatibilities and genomic instabilities (Ding & Chen, 2018; Glombik et al., 2020; Song & Chen, 2015; Svačina et al., 2020; Yoo et al., 2014). These challenges encompass chromosomal rearrangements, mitotic and meiotic abnormalities, and genome-wide gene expression alterations affected by epigenetic responses to the novel genomic constitution (Glombik et al., 2021; Kopecky et al., 2009; Majka et al., 2023; Svačina et al., 2020). One of the challenges for newly arising polyploids is the disruption of stoichiometry between nuclear- and organelle-encoded genes (Ceriotti et al., 2022; Fernandes Gyorfy et al., 2021; Ferreira de Carvalho et al., 2019; Gong et al., 2012, 2014; Li et al., 2020, 2022; Sehrish et al., 2015; Sharbrough et al., 2017; Wang et al., 2017; Zhai et al., 2019). Core functions in eukaryotes depend on the integration and coevolution of nuclear and organelle genomes, particularly within multi-subunit enzyme complexes (Rand et al., 2004; Roux et al., 2016; Woodson & Chory, 2008). Major enzymes in mitochondria and plastids, such as oxidative phosphorylation complexes, photosynthetic machinery, and ribosomes, are assembled using gene products of both nuclear and cytoplasmic genomes. Notably, cytoplasmic RNAs and nuclear-encoded proteins interact extensively, governing posttranscriptional processes, such as intron splicing, transcript end-processing, and RNA editing (Germain et al., 2013). So intimate are these interactions that nuclear and organelle genes, whose products together form protein complexes, exhibit correlated changes in rates of sequence evolution across a phylogeny (so-called evolutionary rate covariation; Forsythe et al., 2021). Thus, co-evolution and communication between individual genomes within the cell are required for plant function and fitness.

Genome-wide changes resulting from polyploidization and hybridization can disrupt the well-tuned stoichiometry between nuclear- and organelle-encoded genes. While WGD doubles the number of nuclear-encoded genes, organelle numbers may not increase proportionally. For instance, tetraploid accessions of *Triticum monococcum* and *Aegilops tauschii* have only 1.5–1.6 times more chloroplasts than diploids (Pyke & Leech, 1987). Similarly, sugar beet after chromosome doubling shows about a 72% increase in chloroplast number (Mochizuki & Sueoka, 1955). These observations raise questions about the impact of nuclear genome doubling on the stoichiometry of chimeric protein complexes. How does inter-genome coordination compensate for the nuclear genome doubling? Are there more copies of chloroplast DNA (cpDNA) or mitochondrial DNA (mtDNA) in each organelle, enhanced expression of organelle-encoded genes, or reduced expression of nuclear-encoded genes in chimeric protein complexes in tetraploids compared to diploids? Or do the organelle-targeted nuclear genes turn to the diploid-like state by pseudogenization/fractionation of the additional copy(ies)? So far, the understanding of these processes in polyploids is limited.

In some polyploids, doubling of the nuclear-encoded gene copies involved in the cytonuclear interactions is not fully compensated by a corresponding doubling of the plastid gene copies (Oberprieler et al., 2019). Autotetraploid *Arabidopsis thaliana*, for example, is able to counteract the effects of the doubled nuclear genome by similarly increasing the number of copies of mitochondrial genes but displays only partial increase of the plastid gene copy number. These observations, however, are based only on quantitative PCR measurements of a single mitochondrial and a single chloroplast gene (Coate et al., 2020). Fernandes Gyorfy et al. (2021) demonstrated an increase in both mitochondria and plastid genome copy numbers per cell in allopolyploid wheat as well as in *Arabidopsis suecica* compared to their diploid relatives. Furthermore, they suggest overcompensation for WGD in tetraploid *Triticum turgidum*. Transcriptional coordination between nuclear- and organelle-encoded genes may vary across ploidy levels, with more conserved coordination observed for plastid compared to mitochondrial genes (Coate et al., 2020). Interestingly, plastid genomes generate 70–80% of all mRNA in the cell, and this abundance is not significantly altered in polyploids (Forsythe et al., 2022). Such abundance is reflected by a 10-fold lower amount of transcripts of the chloroplast-targeted nuclear genes involved in cytonuclear complexes compared to the amount of transcripts of the plastid genes involved in the complexes. Nonetheless, interacting organelle and nuclear genes show strong expression correlation across functional categories, and thus, mRNA stoichiometric imbalance is evidently feasible for the coordinated expression of the cytonuclear complexes (Forsythe et al., 2022).

Cytonuclear interactions in allopolyploids and interspecific homoploid hybrids may also face challenges due to the typical uniparental inheritance of cytoplasmic genomes. Organelle-encoded genes primarily originate from a single parent (usually maternal), while nuclear-encoded genes come from both parents (Birky, 1995; Greiner et al., 2015). Observations on RuBisCO, a single plastid-nuclear complex, provide insights into how parent-specific divergence in nuclear-encoded genes can result in preferential expression of the maternal allele, affecting its retention over time (Gong et al., 2014; Li et al., 2019, 2020; Sehrish et al., 2015). The entire process of the RuBisCO maturation involving folding and assembly stages is further complicated by the necessary involvement of

nuclear-encoded chaperones and chaperonins (Li et al., 2022; Xia et al., 2020). A broad analysis of the cytonuclear accommodation in six allopolyploid lineages by Grover et al. (2022) found cytonuclear genes in most lineages that are biased towards the homoeologue or the expression level from the donor of the cytoplasmic genome. However, the results were not consistent across the lineages or categories of the organelle-targeted genes, and the parent-specific divergence of the genes was not considered.

Studying cytonuclear interactions in polyploids is a captivating area in plant evolutionary biology. Recent advances in genomic and molecular techniques offer unprecedented opportunities to investigate this phenomenon in considerable detail. Understanding the mechanisms governing these interactions and their contribution to the evolutionary relevance of polyploidization may improve our knowledge regarding plant speciation and adaptation to changing environments. Our study, which focused on the chloroplast-nuclear complexes in the *Festuca* and *Lolium* species, including auto- and allopolyploids as well as advanced and newly established generations, sheds light on these changes. We found that stoichiometry restoration after WGD mainly results from an increase in chloroplast DNA (cpDNA) copy number. Additionally, allopolyploid and homoploid *Festuca-Lolium* hybrids display strict maternal inheritance of chloroplasts, with the nuclear component of protein complexes mostly expressed equally from both parental copies.

RESULTS

Chloroplast numbers increase after whole-genome duplication

First, we investigated changes in cell morphology after WGD in the diploid-polyploid complexes of *F. pratensis* and *L. multiflorum*. In *F. pratensis*, we produced autotetraploid plants from diploid cultivars by colchicine treatment. This allowed a direct comparison of diploids vs. autotetraploids (hereafter called newly established autopolyploids) of the same genetic background. In addition, we compared five diploid and five autotetraploid cultivars (hereafter called well-established autotetraploids). In *L. multiflorum*, we used five diploid and five autotetraploid cultivars. Using newly established (C_0 generation) and well-established (~C_8 generation) autopolyploids of *F. pratensis*, we were able to elucidate the changes after several generations of sexual reproduction. Similarly, by using two different species, *F. pratensis* and *L. multiflorum*, we were able to test the species-specificity of the changes associated with WGD.

We used five individuals of each genotype to measure the following parameters: cell volume, nucleus volume, chloroplast volume, and chloroplast number (Figure 1). The cell volume increased by 21% in newly established autotetraploid *F. pratensis*, by 26% in well-established autotetraploid *F. pratensis*, and by 35% in well-established autotetraploid *L. multiflorum* (P value <0.0001; Figure 1a). The volume of nuclei increased by 56%, 71%, and 67% in newly established and well-established *F. pratensis* and *L. multiflorum* autotetraploids, respectively (P value <0.0001; Figure 1b). Thus, nuclear volume increased proportionally more than did cell volume.

All polyploid plants showed a significantly higher number of chloroplasts per cell (p value <0.0001). On average, there were 15%, 35%, and 20% more chloroplasts per cell in newly and well-established *F. pratensis*, and in *L. multiflorum* autopolyploids, respectively, compared to the corresponding diploid plants (Figure 1c). Specifically, newly established autopolyploid *F. pratensis* contained 24 ± 0.27 (mean ± SE) chloroplasts per cell compared to 21 ± 0.3 in corresponding diploid plants from which they originated (diploid plants were cloned and half of the clones were polyploidized; thus, the genotype of diploids and newly established autopolyploids is the same – except genome doubling). Well-established polyploid *F. pratensis* had 34 ± 0.3 chloroplasts per cell compared to 25 ± 0.27 in corresponding diploids; polyploid *L. multiflorum* had 34 ± 0.32 chloroplasts per cell compared to 29 ± 0.29 in diploid *L. multiflorum*. These results indicate that an increase in the number of chloroplasts only partially compensates for the imbalance in the cytonuclear stoichiometry following nuclear genome doubling. The newly established and well-established *F. pratensis* polyploids suggest an immediate response of the plant to WGD but changes become greater in successive generations.

In contrast, we observed only a small increase (but statistically significant; $P < 0.0001$) in the volume of chloroplasts in newly established *F. pratensis* autopolyploids; after this initial increase, the volume appears to return to the diploid-like levels, as seen in well-established *F. pratensis* autopolyploids (only 10% increase; P value = 0.312). In *L. multiflorum*, the volume of chloroplasts in autopolyploids was even smaller than in diploids (by 9%; P value <0.05; however, the effect on the population was small according to Cohen's D test; Figure 1d).

Number of chloroplast genome copies per cell is at least two-fold higher in autopolyploids compared to diploids

To estimate how chloroplast genome copy number changes in response to WGD, we selected three chloroplast-encoded genes involved in three different cytonuclear complexes: *ATP synthase subunit I (ATPI)*, *Photosystem II D2 protein (PSBD)*, and *Ribulose bisphosphate carboxylase large chain (RBCL)*, measured their copy number by droplet digital PCR (ddPCR) and compared the results between the polyploid and the corresponding diploid plants. The same sets of *F. pratensis* and *L. multiflorum* diploid and autotetraploid plants were analyzed as described above. We used a

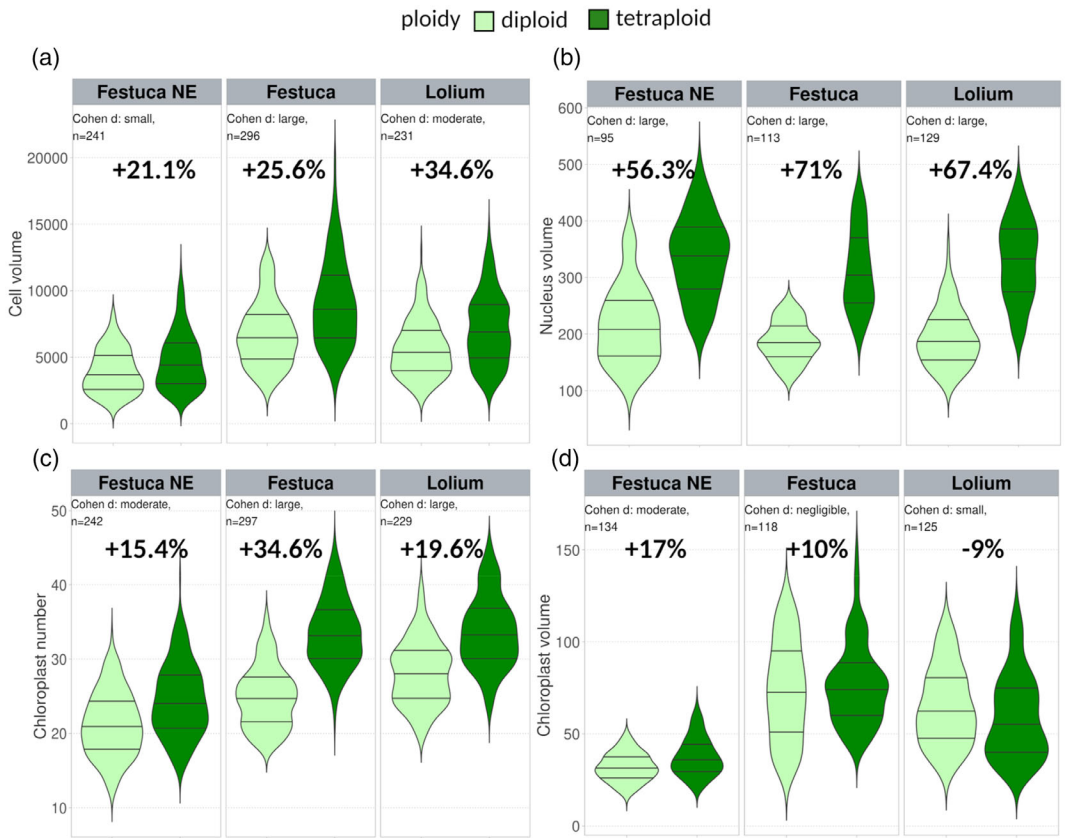

Figure 1. Changes in leaf cell morphology after WGD in *F. pratensis* and *L. multiflorum*. *y*-axis represents cell volume (a); nuclear volume (b); the number of chloroplasts (c) and chloroplast volume (d). Mean differences between diploids (light green) and tetraploids (dark green) are expressed as +% for an increase in the tetraploid and −% for a decrease in the autotetraploid. The effect size of the difference between the two means is represented by Cohen's D test. Negligible effect $d < 0.2$; small effect $d = 0.2–0.5$; moderate effect $d = 0.5–0.8$; large effect $d \geq 0.8$; NE, newly established; n, number of cells evaluated.

single-copy nuclear gene *actin 2* (*ACT2*) to estimate the number of nuclei in a sample by dividing the *ACT2* copy number per sample by the ploidy of the sample. Although the analysis could potentially be biased by endopolyploidy, flow cytometry did not identify endopolyploid nuclei (8C DNA amount) in the samples of both, diploids and autotetraploids. The results showed that the copy number of the chloroplast genome was higher in all polyploids examined compared to diploids. Newly established *F. pratensis* polyploids contained 258 ± 17 (mean ± SE) vs. 122 ± 11 copies per cell in corresponding diploids (Figure 2a). Advanced generation polyploid *F. pratensis* plants showed an even greater increase over their diploid counterparts: 1543 ± 126 vs. 583 ± 56 (Figure 2b) per cell. *Lolium multiflorum* polyploids had 1202 ± 95 copies, while diploids had 485 ± 53 copies per cell (Figure 2c). Overall, an increase in well-established *F. pratensis* and *L. multiflorum* polyploids was 2.5-fold (*P* value <0.05; the effect size based on Cohen's D test = large in all per gene pairwise comparisons), while in newly established *F. pratensis* polyploids, it was 2.1-fold (*P* value <0.05; effect size based on Cohen's D test = large in all per gene pairwise comparisons). Our data suggest that the imbalance in cytonuclear complexes after WGD is fully compensated or even overcompensated by increasing the number of copies of the chloroplast genome. This is achieved through both increasing the number of chloroplasts (minor effect) and increasing the number of genomes per chloroplast (main contributor). We observed that polyploids responded to WGD by an instant increase in the chloroplast genome copies and carried on with modifications (further increase) in subsequent generations.

Only marginal changes in gene expression after polyploidization

We used qPCR to evaluate changes in the expression of chloroplast and nuclear genes involved in cytonuclear complexes after WGD (Figure 3). We used autotetraploid cultivars and compared them with diploid cultivars (the same as those used in morphological and cpDNA copy number analyses). To normalize the qPCR data at each ploidy level and thereby account for the increased expression due to the higher number of chloroplast genomes present in polyploids compared to diploids, we used constitutively expressed gene *maturase K* (*MATK*) as the

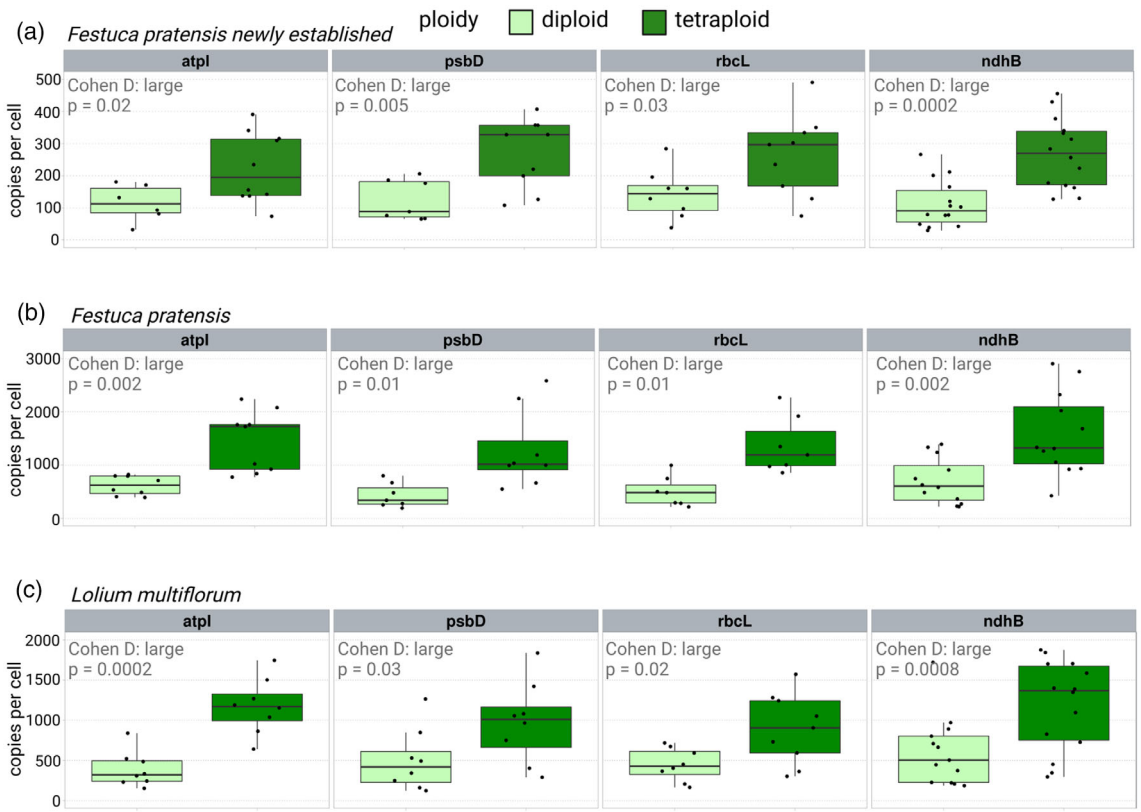

Figure 2. Changes in chloroplast gene copy number after WGD in leaves of *F. pratensis* and *L. multiflorum*. Each plot represents the number of chloroplast genome copies in diploid (light green) and corresponding autotetraploid (dark green) plants based on ddPCR of several chloroplast encoded genes in newly established (a) and well-established autotetraploid *F. pratensis* (b) and well-established autotetraploid *L. multiflorum* (c). The *y*-axis represents a number of gene copies per cell. Chloroplast gene *NAD(P)H-quinone oxidoreductase subunit 2* (*NDHB*) has been included as a control. Its values were divided by two because it has two copies per chloroplast genome. The effect size of the difference between the two means is represented by Cohen's D test. Negligible effect $d < 0.2$; small effect $d = 0.2$–0.5; moderate effect $d = 0.5$–0.8; large effect $d \geq 0.8$.

chloroplast reference gene and *ACT2* and *eukaryotic initiation factor 4A* (*EIF4A*) as the reference genes for nuclear transcripts. The transcript abundance measurements revealed that an increase in ploidy level from diploid to tetraploid in *F. pratensis* led to a slight increase in the expression level of all three chloroplast genes (*ATPI*, *PSBD*, and *RBCL*). There was a slight reduction in the expression level of the two nuclear genes (*ATPC1* and *RBCS*) and a slight increase of the one nuclear gene (*PSBR*), but none of these changes were statistically significant (Figure 3a). An increase in the ploidy level of *L. multiflorum* had no large effect on the expression levels of genes associated with cytonuclear complexes; some of the genes displayed a slight increase whereas others showed a slight decrease (Figure 3b). Taking into account the altered copy number, WGD has only a marginal effect on the overall expression levels of the genes (both nuclear and chloroplast) involved in cytonuclear complexes.

Maternal inheritance of chloroplasts in the hybrids

An intriguing question concerned preferential expression (homoeologous expression bias; HEB) of parental alleles of nuclear genes in allopolyploid and homoploid hybrids and the overall expression of these genes in both types of hybrids compared to the expression in their parents (expression level dominance; ELD; Grover et al., 2012). In cases of maternal inheritance of the chloroplast genome, one might hypothesize a preferential expression of maternal alleles of the nuclear genes involved in cytonuclear complexes, and secondly, that expression levels of these genes might be similar to that of the maternal parent.

First, we investigated the inheritance pattern of the chloroplasts in our available hybrids: reciprocal tetraploid *L. multiflorum* × *F. pratensis* and *F. pratensis* × *L. multiflorum* and diploid *L. perenne* × *F. pratensis*. The reason for using diploid *L. perenne* × *F. pratensis* hybrids was to compare expression patterns in diploid (homoploid) hybrids vs. allopolyploids. Sequencing of two chloroplast genes (*ATPI* and *PSBD*) from both parents (*L. multiflorum* and *F. pratensis*) allowed us to identify single nucleotide polymorphisms (SNPs) in both genes, which discriminated alleles of both parents. Using Sanger sequencing, we revealed the maternal inheritance pattern in all homoploid and allotetraploid hybrids (Table 1; Figure S1).

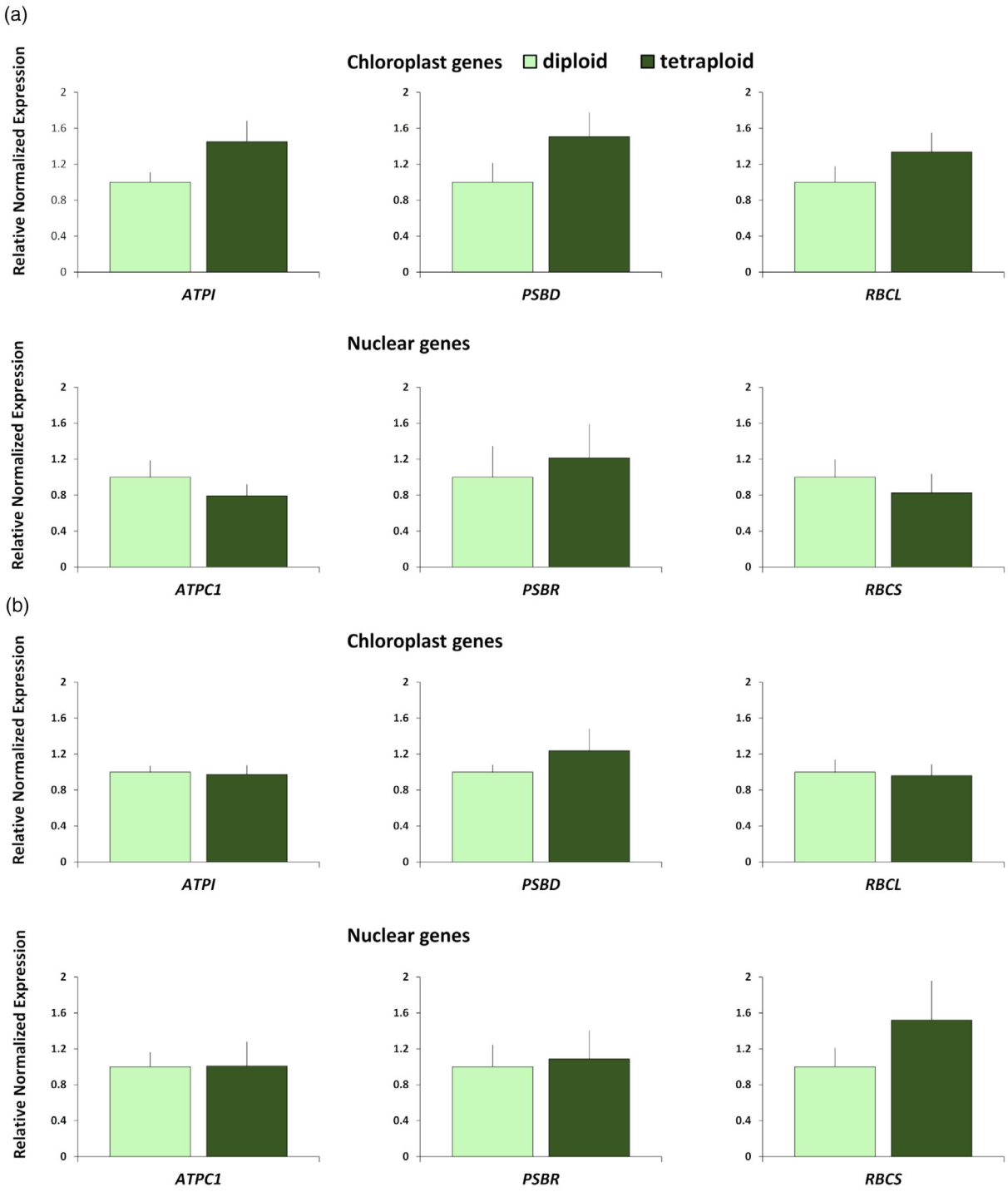

Figure 3. Relative transcript abundance of chloroplast *ATPI, PSBD*, and *RBCL* and nuclear *ATPC1* (*ATP synthase gamma chain 1*), *PSBR* (*Photosystem II 10 kDa polypeptide*) *RBCS* (*Ribulose bisphosphate carboxylase small subunit*) genes involved in cytonuclear complexes in *F. pratensis* (a) and *L. multiflorum* (b). Error bars represent the standard error of the mean of the biological replicates (n = 5).

Expression level dominance (ELD) of nuclear genes involved in cytonuclear complexes

Next, we investigated whether the maternal inheritance of the chloroplast genome is reflected in the maternal ELD of nuclear genes involved in cytonuclear complexes; that is, whether the overall expression level (summed from both parental alleles) of these genes in hybrids is the same as in the maternal parent but different from the expression

Table 1 Determination of the chloroplast inheritance pattern in homoploid (2*x*) and allotetraploid (4*x*) reciprocal hybrids of *Lolium* × *Festuca* and *Festuca* × *Lolium* using Sanger sequencing of chloroplast genes (*ATPI* and *PSBD*). Nuclear gene *ATPC1* was used as a control. *Lm and Lp* represents *L. multiflorum* and *L. perenne* inheritance of the gene, *Fp* represents *F. pratensis* inheritance

Sample (ploidy)	*ATPC1*	*ATPI*	*PSBD*
F. pratensis × *L. multiflorum* 10/2 (4*x*)	*Fp* + *Lm*	*Fp*	*Fp*
F. pratensis × *L. multiflorum* 10/4 (4*x*)	*Fp* + *Lm*	*Fp*	*Fp*
F. pratensis × *L. multiflorum* 10/6 (4*x*)	*Fp* + *Lm*	*Fp*	*Fp*
F. pratensis × *L. multiflorum* 10/7 (4*x*)	*Fp* + *Lm*	*Fp*	*Fp*
F. pratensis × *L. multiflorum* 10/8 (4*x*)	*Fp* + *Lm*	*Fp*	*Fp*
L. multiflorum × *F. pratensis* 5/1 (4*x*)	*Fp* + *Lm*	*Lm*	*Lm*
L. multiflorum × *F. pratensis* 5/2 (4*x*)	*Fp* + *Lm*	*Lm*	*Lm*
L. perenne × *F. pratensis* 3/3 (2*x*)	*Fp* + *Lp*	*Lp*	*Lp*
L. perenne × *F. pratensis* 5/3 (2*x*)	*Fp* + *Lp*	*Lp*	*Lp*
L. perenne × *F. pratensis* 6/7 (2*x*)	*Fp* + *Lp*	*Lp*	*Lp*
L. perenne × *F. pratensis* 7/5 (2*x*)	*Fp* + *Lp*	*Lp*	*Lp*
L. perenne × *F. pratensis* 8/2 (2*x*)	*Fp* + *Lp*	*Lp*	*Lp*

level of the paternal parent. We interrogated the RNA-seq data of reciprocal allotetraploid *L. multiflorum* × *F. pratensis* hybrids and their parents from our previous study (Glombik et al., 2021). We selected nine nuclear genes involved in the cytonuclear complexes for which we could distinguish both parental alleles based on SNPs and analyzed their expression (Table 2). The selected genes included: *ATPC1*, photosystem II involved *PSBW*, chaperonins *CPN60A* involved in the RuBisCO complex assembly and the *YL1* assembly factor involved in the ATP synthase complex assembly and the photosystem II related *LPA1* chaperone, the *HCF136* stability/assembly factor and the *PPL1* which facilitates the assembly of photosystem II complex. Based on the comparison of the total expression levels of homoeologous gene pairs in the hybrids to the expression levels in their two parents, we assigned genes to one of the 13 ELD categories previously described by Rapp et al. (2009). There were five biological and three technical replicates for both types of hybrids and three technical replicates of parents (only one *Lolium* and one *Festuca* plant were used to generate the allotetraploids).

In the ATP synthase complex, nuclear gene *ATPC1* was upregulated (class VIII; Rapp et al., 2009, here and below) in both reciprocal hybrids compared to the parents, and its chaperonin *YL1* demonstrated the *Lolium* expression level dominance (class XI) pattern in both directions of the cross. From the RuBisCO complex, chaperonin *CPN60A* also showed the *Lolium* expression level dominance in both reciprocal hybrids (class XI). Thus, RuBisCo and the ATP synthase complexes displayed similar patterns.

In the photosystem II complex, the nuclear gene *PSBW* was upregulated (class V) in *F. pratensis* × *L. multiflorum* compared to the parents and displayed maternal (*Lolium)* ELD (class II) in *L. multiflorum* × *F. pratensis* hybrids. The assembly factors related to the photosystem II complex demonstrated different patterns of ELD. *LPA1* exhibited maternal ELD (class IV) in *F. pratensis* × *L. multiflorum* and upregulation (class VI) in *L. multiflorum* × *F. pratensis* hybrids compared to the parents. The *HCF136* was upregulated (class VIII) in *L. multiflorum* × *F. pratensis* compared to both parents. In *F. pratensis* × *L. multiflorum* hybrids, it was not possible to assign unambiguously this gene to a particular ELD category, and was considered as 'unassigned' (UC). Lastly, *PPL1* was upregulated (class VIII) in *F. pratensis*× *L. multiflorum* compared to the parents and an unassigned category in *L. multiflorum*× *F. pratensis*. Overall, we detected different categories of ELD with

Table 2 ELD of nuclear genes involved in cytonuclear complexes and related chaperonins and chaperones in reciprocal hybrids based on RNAseq data

	RuBisCO complex	RuBisCO Complex assembly	ATP synthase complex	ATP synthase complex assembly	Photosystem II complex		Photosystem II complex assembly		
Complexes	*RBCS*	*CPN60A*	*ATPC1*	*YL1*	*PSBW*	*PSBR*	*HCF136*	*LPA1*	*PPL1*
F_1 F×L	UC	XI LED	VIII tr_up	XI LED	V tr_up	UC	UC	IV FED	VIII tr_up
F_1 L×F	UC	XI LED	VIII tr_up	XI LED	II LED	UC	VIII tr_up	VI up	UC

UC, unassigned category; FED, *Festuca* expression dominance; LED, *Lolium* expression dominance; tr_up, transgressive upregulation; tr_down, transgressive downregulation.

no obvious relationship to the inheritance pattern of the chloroplast genome, with the exception of *PSBW* and *CPN60A* with maternal ELD in *L. multiflorum* × *F. pratensis* and *LPA1* with maternal ELD in *F. pratensis* × *L. multiflorum*.

Homoeolog expression bias (HEB) of nuclear genes involved in cytonuclear complexes

The same set of RNA-seq data as above was used to determine the HEB of the previously selected genes (Table 3), to test the hypothesis that the chloroplast-targeted nuclear genes should display HEB towards the chloroplast genome donor (maternal in our case). HEB refers to the phenomenon, where homoeolog from one parental genome contributes to the expression of the particular gene significantly more than the homoeolog from the other parental genome. The analysis showed that for *RBCS*, *ATPC1*, *PSBW*, *PSBR*, *YL1*, *HCF136*, and *PPL1* genes, the contribution of alleles from both parental genomes was equal (statistically not different based on the t-test). Interestingly, *PSBW* demonstrated *L. multiflorum*-biased expression (L > F) but only in aging leaves of F_2 generation of *F. pratensis* × *L. multiflorum* hybrids (Table S1).

CPN60A demonstrated maternal HEB in *F. pratensis* × *L. multiflorum* hybrids but equal expression from both parents in *L. multiflorum* × *F. pratensis*. *LPA1* was more highly expressed by *F. pratensis* in *L. multiflorum* × *F. pratensis* (paternal HEB) and equally expressed by both parental subgenomes in *F. pratensis* × *L. multiflorum* hybrids. Finally, the control gene *PPD7* (PSBP domain-containing protein 7), which is part of the chloroplast lumen thylakoid but is not involved in cytonuclear complexes or related assembly factors, was preferentially transcribed from the *L. multiflorum* subgenome-derived allele in both reciprocal hybrids. To confirm the RNA-seq data, quantitative Sanger (qSanger) sequencing was used for three nuclear genes (*ATPC1*, *PSBR*, and *PPD7*; Figure 4). There was no statistically significant difference in *ATPC1* (Figure 4a) and *PSBR* (Figure 4b) expression levels in either reciprocal hybrid, although *ATPC1* expression from the *Lolium* allele was slightly higher than from the *Festuca* allele. The qSanger results further confirmed a significantly higher expression of *PPD7* from the *Lolium* allele compared to the *Festuca* allele (Figure 4c). Expression was about nine-fold higher in both *F. pratensis* × *L. multiflorum* and *L. multiflorum* × *F. pratensis* polyploids. Having access to homoploid hybrids, we also performed qSanger on five homoploid *L. perenne* × *F. pratensis* plants (F_1 generation). Similar to allotetraploids, *ATPC1* and *PSBR* did not show statistically significant differences in the contribution of parental alleles, whereas *PPD7* had three-fold higher expression from the *Lolium* allele compared to the *Festuca* allele (Figure S2, Table S2). Altogether, we did not detect any consistent pattern of HEB in the chloroplast-targeted genes that would follow the pattern of chloroplast inheritance.

Table 3 Homoeolog expression bias (HEB) of nuclear genes involved in cytonuclear complexes and related chaperonins and chaperones in reciprocal hybrids based on RNAseq data

Complex	Gene	F_1 F×L	F_1 L×F
RuBisCO complex	RBCS	F = L	F = L
RuBisCO assembly	CPN60A	F > L	F = L
ATP synthase complex	ATPC1	F = L	F = L
ATP synthase assembly	YL1	F = L	F = L
Photosystem II complex	PSBW	F = L	F = L
	PSBR	F = L	F = L
Photosystem II assembly	HCF136	F = L	F = L
	LPA1	F = L	F > L
	PPL1	F = L	F = L
Control gene	PPD7	L > F	L > F

Structural conflicts

Considering that there was no homoeolog expression bias towards the donor of the chloroplast genome for a majority (eight out of nine) of the genes tested, we hypothesized that the homoeologous proteins are structurally identical and hence functionally interchangeable. In contrast, the genes with HEB might be structurally divergent between the parental alleles (*Lolium* and *Festuca*). To test this, we selected three genes (*PSBW, CPN60A*, and *LPA1*) with HEB in at least one of the analyzed genotypes and compared their protein structure. Coding sequences of these genes were obtained from transcriptomes of both species generated in our previous study (Glombik et al., 2021) and translated into the corresponding amino acid sequences. This showed several non-synonymous SNPs present altering the amino acid sequences (3, 2, and 2 altered amino acids for PSBW, CPN60A, and LPA1, respectively). We further investigated the impact of these SNPs on protein function and protein–protein interactions. We developed a pipeline to study the potential consequences of amino acid variation on the protein structure and the electrostatic potential of the binding sites. This pipeline involved the identification of the functional domains of the proteins and multiple-sequence alignment with at least 20 closely related homologs to determine both the highly conserved amino acids and mutations within the functional domains. We found that PSBW, containing the PsbW superfamily domain (21–127 a.a.), has amino acid substitutions between *Festuca* and *Lolium* (Fp*Lm), at three codons (14-Thr*Ala), (37-Ala*Ser), and (39-Cys*Ser), located in unstructured parts of the protein (Figure 5a, Table 4). Considering the physico-chemical properties of the substituted amino acids (Gasteiger et al., 2003), the substitution of Ala (non-polar) with Thr (polar), Ala (non-polar) with Ser (polar), and Cys (non-polar) with Ser (polar) may potentially change the polarity of the protein and affect protein–protein interactions. Substitution of Thr with Ala can affect

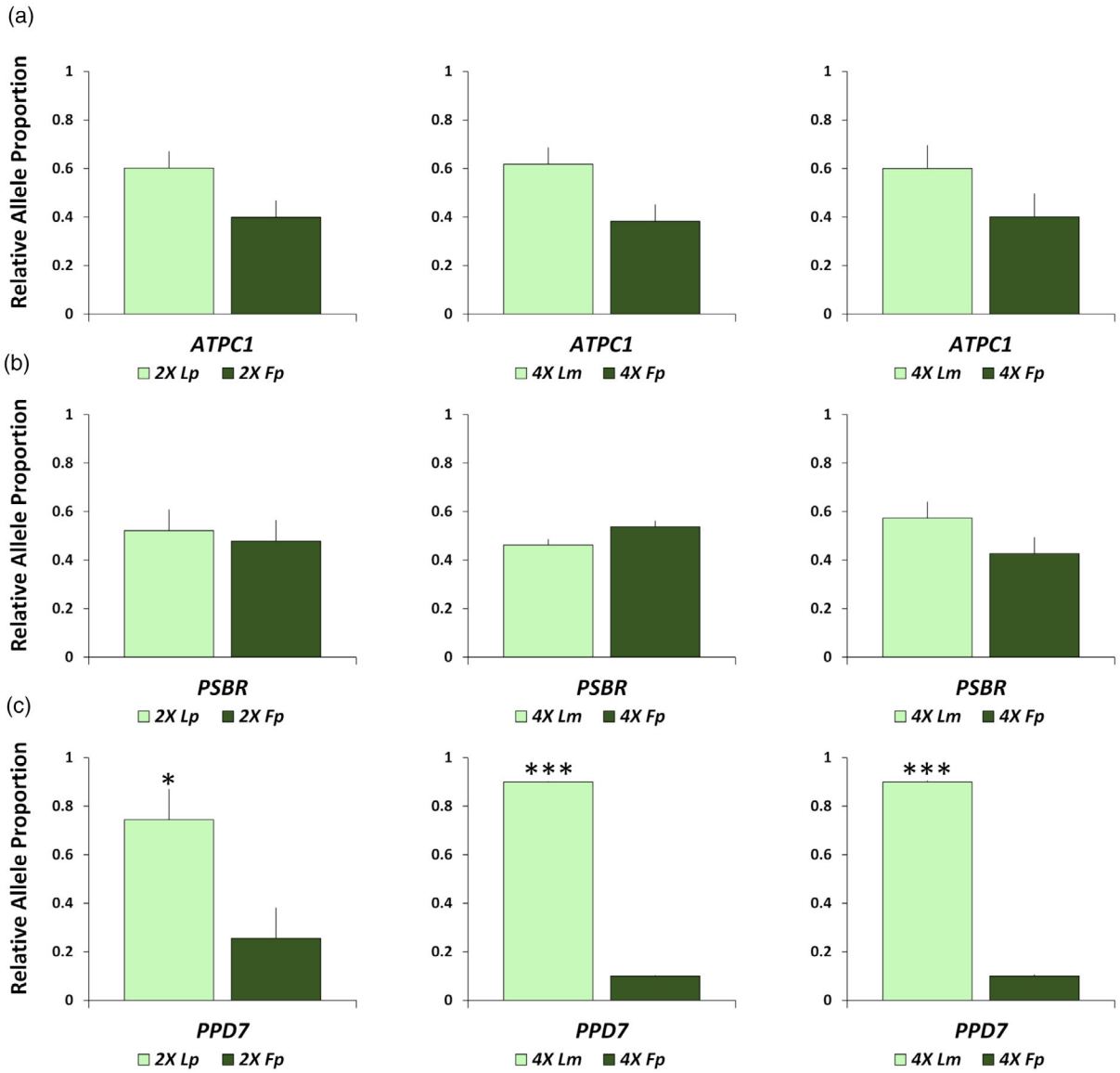

Figure 4. Homoeolog expression bias (HEB) of nuclear genes involved in cytonuclear complexes. *ATPC1* (a), *PSBR* (b), and *PPD7* (c) in homoploid *L. perenne* × *F. pratensis* (left) and allotetraploids *F. pratensis* × *L. multiflorum* (middle), and *L. multiflorum* × *F. pratensis* (right). Note the overexpression of the *Lolium* allele of *PPD7* in all three hybrids. Error bars represent the standard error of the mean of the biological replicates. *** $P < 0.001$, * $P < 0.05$ (Based on two-tailed Student's *t*-test).

local folding and interactions because Thr has a hydroxyl group and a larger side chain than Ala, which is highly hydrophobic and typically found in the hydrophobic core of the protein. Replacing Cys with Ser can significantly affect protein local stability and folding. This is because Cys contains a sulfhydryl group that contributes to redox reactions and disulfide bond formation, while Ser is polar and has hydroxyl groups that facilitate water interactions and hydrogen bonding. Additionally, the hydroxyl groups of Ser allow it to participate in hydrogen bonding and interact with functional groups. Measurements of the electrostatic potential of the surface demonstrated that substitution of Thr with Ala may decrease the local electrostatic potential, and with the substitution of Ala with Ser, an increase in the surface electrostatic potential is possible (Figure 6a). Finally, substitution of Cys with Ser may lead to a decrease in the electrostatic potential of the region. Overall, changes in the amino acid sequence can change the shape, charge, and polarity of the protein and influence the efficiency of the interactions between the subunits of photosystem II in hybrids. This is a promising direction for future research.

CPN60A, containing a GroEL-like domain (52–572 a.a.), also demonstrated variation in amino acid sequences

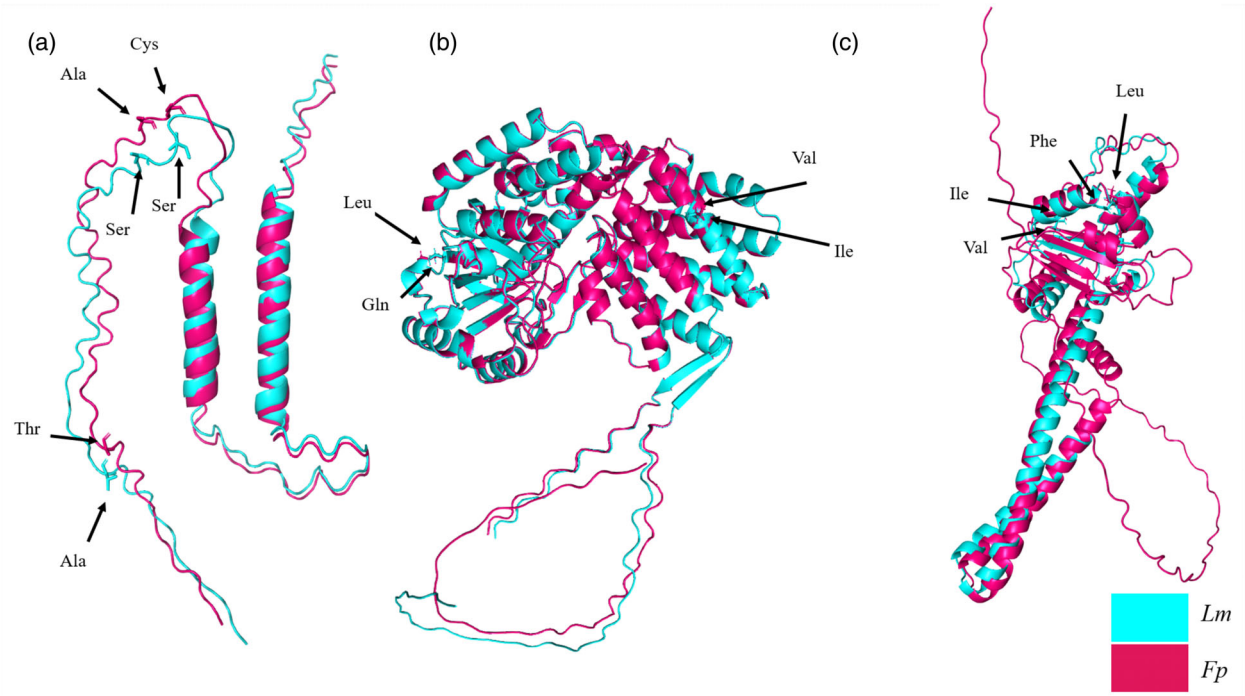

Figure 5. Predicted protein structures of Festuca and Lolium variants of the genes exhibiting HEB (a) Superimposition of PSBW from Festuca (hot pink) and Lolium (cyan) variants, (b) Superimposition of CPN60A from Festuca (hot pink) and Lolium (cyan) variants, and (c) Superimposition of LPA1 from Festuca (hot pink) and Lolium (cyan) variants. The protein structure predictions were generated by AlphaFold2 (Jumper et al., 2021).

Table 4 Functional domain sites, detected amino acid differences and the subsequent effects on protein structure between *Festuca (Fp)* and *Lolium (Lm)* variants of PSBW, CPN60A, and LPA1

Gene name	Functional domain site	Detected amino acid differences	Structural effect of the amino acid substitutions
PSBW Fp PSBW Lm	21–127 21–127	(14-Thr), (37-Ala), (39-Cys) (14-Ala), (37-Ser), (39-Ser)	• Altering local hydrophobicity and folding • Facilitating hydrogen bonding, • Influencing stability through redox reactions and disulfide bond formation.
CPN60A Fp CPN60A Lm	52–572 49–569	(172-Gln), (366-Ile) (172-Leu), (366-Val)	• Altering local hydrophobicity • Facilitating hydrogen bonding,
LPA1 Fp LPA1 Lm	94–341 94–341	(218-Ile), (228-Phe) (218-Val), (228-Leu)	• Altering local hydrophobicity and folding

(Fp*Lm), (172-Gln*Leu), and (366-Ile*Val) in highly conserved regions of the sequence (Figure 5b). The substitution of Gln (polar) with Leu (non-polar) changes the polarity and can promote hydrogen bonding due to Gln amide group. Leu is highly hydrophobic favoring interactions within protein cores. Both Ile and Val are non-polar amino acids with aliphatic side chains, contributing to hydrophobic interactions in protein structures. The listed substitutions can potentially change the shape of the protein (Figure 6b). Substitution of Gln with Leu may also result in a decrease in the local electrostatic potential. For Ile and Val, both amino acids have similar electrostatic properties.

The functional domain of LPA1 (94–341), showed an amino acid insertion of Ala, Val, and Ser in the *Lolium* variant and an insertion of Ala and Val in the *Festuca* variant. The detected substitutions (Fp*Lm), (218-Ile*Val), and (228-Phe*Leu) were found inside the functional domain and highly conserved parts of the proteins (Figure 5c, Table 4). These substitutions will change the structural shape (Figure 6c) and affect the interactions. However, the polarity is not altered as both substitutions are from non-polar to non-polar amino acids. As mentioned above, Ile and Val feature aliphatic side chains, predominantly engaging in hydrophobic interactions. Phenylalanine's (Phe) aromatic ring intensifies its hydrophobicity and alters local folding.

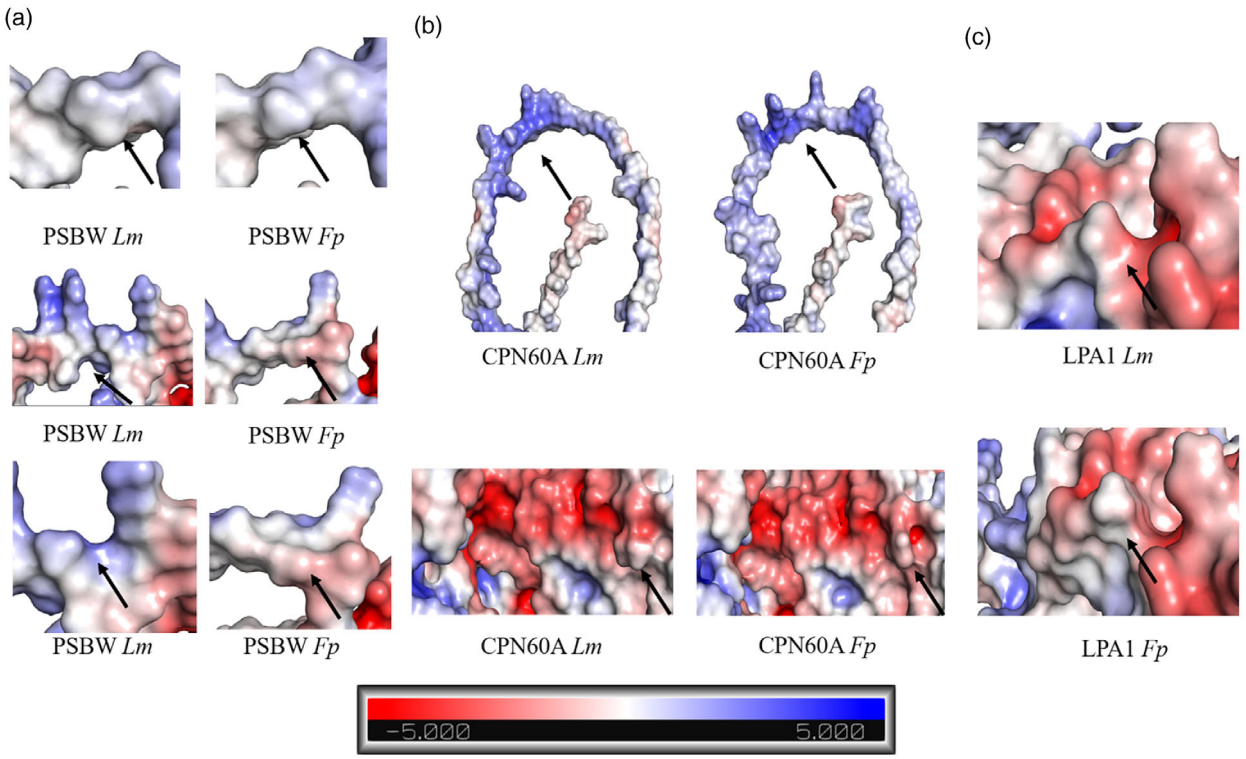

Figure 6. Structural and electrostatic potential differences between Festuca and Lolium variants of the genes exhibiting HEB. (a) PSBW from Festuca (Fp) and Lolium (Lm) variants, (b) CPN60A from Festuca (Fp) and Lolium (Lm) variants, and (c) LPA1 from Festuca (Fp) and Lolium (Lm) variants (white, neutral; blue, $+5kT\ e^{-1}$; red, $-5kTe^{-1}$).

Meanwhile, Leu as a nonpolar amino acid actively participates in hydrophobic interactions.

All three proteins we studied vary in structure between *Festuca* and *Lolium*, raising the possibility that there might be functional differences between the variants. However, the interchangeability of the variants needs to be investigated empirically. Notably, although there are amino acid substitutions between *Lolium* and *Festuca* in the chloroplast-encoded genes for each of these three complexes (Table S3), none of those amino acid changes were at contact residues. Indeed, of the 50 amino acid differences between *Lolium* and *Festuca* (Table S3), none were at contact residues, making it likely that nuclear subunits from either *Lolium* or *Festuca* are capable of working equally well with both chloroplast genomes.

DISCUSSION

The consequences of polyploidization for cytonuclear interactions and the restoration of a well-tuned stoichiometry have been intensively studied in recent years, including the evolutionary rates of homoeologs of the organelle-targeted nuclear genes (Sharbrough et al., 2022), homoeolog expression bias of these genes (Grover et al., 2022) or modifications in organelle genome copy number in polyploids (Coate et al., 2020; Fernandes Gyorfy et al., 2021).

A majority of the research concentrated on a few allopolyploid complexes, usually well-established allotetraploid species with a long history of speciation after the initial hybridization event, such as tetraploid wheat, cotton, and *Brachypodium*. Much of this research focuses on a single process (e.g., biased evolutionary rate of homoeologs of nuclear genes involved in the cytonuclear interactions) and collectively they have provided inconsistent results among species, thus preventing understanding of more general principles that might be true for cytonuclear evolution following polyploidization. Moreover, the literature to date has focused primarily on allopolyploids, with autopolyploids only rarely explored. This is understandable; allopolyploids, with two diverged parental genomes and usually maternally inherited organelles, offer more opportunities to study evolutionary processes accompanying hybridization and genome doubling. On the other hand, inferences derived from comparison of allopolyploids with their putative progenitors are complicated by the different evolutionary histories of diploid progenitors and/or evolved differences between subgenomes subsequent to the allopolyploid formation (Sharbrough et al., 2022). To our knowledge, no one has yet evaluated the contribution of multiple stoichiometric or scaling processes (increase in the number of organelles, increase in organelle DNA copy

numbers, changes in gene expression, etc.) as responses to hybridization and WGD in a single study. Our work provides this perspective for the early generations of auto- and allopolyploids of *L. multiflorum* and *F. pratensis*.

Major trigger of the cytonuclear stoichiometry restoration in polyploid L. multiflorum and F. pratensis is cpDNA copy number increase

Disruption of a well-tuned stoichiometry between nuclear and organelle components of protein complexes is among the most important challenges new polyploids face. While the number of copies of the nuclear genes is doubled after WGD, the number of organelle genes is not increased immediately to a double dose. For example, tetraploid alfalfa and Arabidopsis had 39% and 55% more chloroplasts than diploids, respectively, and a multi-species screen reported a 69% increase in both C_0 and C_1 generations (Bingham, 1968; Butterfass, 1991; Kawade et al., 2013). This is congruent with our study; we found that the number of chloroplasts in autotetraploid cultivars of *F. pratensis* and *L. multiflorum* was higher by 35% and 20%, respectively, compared to their diploid counterparts. Observations of newly created (C_0 generation) and well-established (C_8) autotetraploids of *F. pratensis* suggest that this is not a one-step process, and the number of chloroplasts may increase in successive generations, similar to the increase in cell and nuclear volume. However, it is evident that the increase in the number of organelles does not fully compensate for the doubling of the nuclear genome, and therefore, other factors must act in the stoichiometry restoration.

Various studies have recently addressed changes in cytonuclear interactions after the induction of polyploidy. One of the most studied processes is an increase in organelle DNA copy number (Coate et al., 2020; Fernandes Gyorfy et al., 2021; Oberprieler et al., 2019); however, in these studies, the results have been contradictory across the polyploid complexes studied. Fernandes Gyorfy et al. (2021) reported two to three times more organelle genomes per cell than in the diploids of wheat/*Aegilops* and Arabidopsis. Similarly, here we found that the imbalance in the cytonuclear complexes after WGD is fully compensated (actually, even overcompensated) by an increase of the organelle genome copy numbers in *F. pratensis* and *L. multiflorum*. What makes these two studies different is the inconsistency in the modification of the organelle genome copy number over generations. Our study shows a continuous increase of the organelle genome copy number in successive generations (progression from 2.1-fold to 2.5-fold difference between C_0 and C_8) in *F. pratensis*, the same as observed in synthetic autotetraploids and natural allotetraploid of Arabidopsis. In both of these di-/tetraploid complexes, Arabidopsis and *F. pratensis*, compensation by an increase in the organelle genome copy number occurs immediately with the onset of WGD. In *F. pratensis*, the balance between the organelle and nuclear parts of the chimeric cytonuclear protein complexes is further tuned in successive generations. However, not all studies point in the same direction. The increase in the number of copies of the nucleus-encoded genes after polyploidization was not fully compensated by an increase in the copy numbers (through an increase in chloroplasts per cell and/or increase in plastid genomes per chloroplast) on the plastid side in autopolyploid *Leucanthemum* and *A. thaliana* (Coate et al., 2020; Oberprieler et al., 2019). In Arabidopsis, the copy number of plastid genes increased by 52% after WGD (Coate et al., 2020).

Another way to restore the stoichiometry between components of the cytonuclear complexes is the down-regulation of nuclear genes and/or up-regulation of the organelle genes (Sharbrough et al., 2017). Slight down-regulation of the chloroplast-targeted nuclear genes (per ploidy) was indeed observed in the nascent autopolyploid *A. thaliana*, generally reflecting the reduction of the cpDNA per cell (Coate et al., 2020). On the contrary, Grover et al. (2022) did not find any evidence of the transgressive upregulation of the organelle-targeted nuclear gene expression that would indicate compensation for the changes in the proportion of the organelle vs. organelle-targeted nuclear genes caused by WGD. Similarly, we found only minor changes in the overall expression of the nuclear (non-significant down-regulation) and organelle (non-significant upregulation) genes.

All these observations suggest that each polyploid complex restores cytonuclear-interaction stoichiometry by similar mechanisms and processes (i.e., elevated cpDNA copy number); however, their relative contributions may be species-specific. Moreover, while the response to WGD is immediate, copy numbers can continue to elevate over successive generations. Thus, the numbers of organelles, organelle genome copy numbers, and the transcriptional activities of both nuclear and organelle genes involved in the cytonuclear complexes may vary between generations. This is not surprising, considering that there may be considerable variation in the number of organelles per cell (here the number of chloroplasts differed two-fold among the cells of the same tissue) and the number of cpDNA molecules (about five- to sixfold difference; sixfold difference in *Aegilops speltoides* by Fernandes Gyorfy et al., 2021) per cell. Thus, one could argue that doubling of organelle-targeted nuclear genes may have little effect on the stoichiometry of the interacting partners. However, it is evident that the organisms react to WGD mainly by increasing the number of organelles and the number of cpDNA molecules in each chloroplast. Thus, polyploidization presumably does not cause an instant significant disruption of the cytonuclear interactions, but evolutionary changes play a role and tune these interactions to the diploid-like stage with a well-tuned stoichiometry of the interacting components from organellar and nuclear genomes.

Biological relevance of ELD and HEB for cytonuclear interactions in allopolyploids

In most allopolyploids and homoploid hybrids, organelles are inherited maternally (Birky, 1995; Greiner et al., 2015). It is strictly so in F_1 hybrids of *L. perenne* × *F. pratensis* and *F. pratensis* × *L. perenne* (Kiang et al., 1994). However, some backcross generations of the initial hybrids had paternally derived chloroplasts and mitochondria. In this study, we showed that only the maternal variant of cpDNA is present in our reciprocal *Lolium* × *Festuca* hybrids. This raises the question of whether there is a bias in preferential retention and upregulation of expression of the maternal allele (maternal HEB) of the organelle-targeted nuclear genes and a bias in the expression of these genes to the level present in the maternal parent (maternal ELD). Contradictory results have been published on the retention of maternal vs. paternal alleles of organelle-targeted nuclear genes in the successive generations of allopolyploids. While there is maternally biased gene conversion in some allopolyploids such as cotton, wheat, and quinoa (Gong et al., 2014; Jarvis et al., 2017; Li et al., 2020; Sharbrough et al., 2022), it has not been found in others, including *Brassica napus* (Ferreira de Carvalho et al., 2019). Gong et al. (2012, 2014) identified maternally biased homoeolog expression levels of the RuBisCO complex in five allopolyploids including *Gossypium* and Arabidopsis. On the other hand, Grover et al. (2022) conducted comprehensive screening of six allopolyploids (*Arabidopsis suecica*, *Arachis hypogea*, *Arachis ipaensis* x *Arachis duranensis*, *Chenopodium quinoa*, *Gossypium hirsutum*, and *Gossypium barbadense*) for both HEB and ELD and found patterns largely inconsistent with cytonuclear expectations (*i.e.*, upregulation of maternal alleles and down-regulation of paternal alleles and the overall expression in allopolyploids generally similar to maternal parent and dissimilar to the paternal parent). Our results show a similar pattern; we observed ELD and HEB in chloroplast-targeted nuclear genes, and the pattern did not agree with the cytonuclear expectations, with the exception of *CPN60A and LPA1* in the *F. pratensis* × *L. multiflorum* hybrid. This lack of consistency is also apparent in other studies; maternal-biased expression was observed in some allopolyploids, but not in others (Shan et al., 2020; Wang et al., 2017; Zhai et al., 2019). In addition, the bias towards maternal alleles, if any, may have evolved within successive generations after the initial hybridization. While the natural populations of *Tragopogon miscellus* and *Brassica napus* show the maternal bias for cytonuclear-related genes, synthetically derived individuals may not follow this pattern (Ferreira de Carvalho et al., 2019; Sehrish et al., 2015; Shan et al., 2020).

One might also ask what is the biological relevance of the parental-allele biased expression of organelle-targeted nuclear genes with respect to cytonuclear interactions. In case of ELD, the expectation of maternally biased expression is logical (considering maternally inherited organelles), however, HEB has the biological relevance only if the two parental copies functionally differ. Even though there are a number of reports describing HEB in plant hybrids and allopolyploids, including those dealing with cytonuclear interactions (Ferreira de Carvalho et al., 2019; Grover et al., 2022; Shan et al., 2020), only a few address differences of the gene variants and their consequences for the proper assembly of the chimeric complexes. Abdel-Ghany et al. (2022) studied sequence variability of the plastid caseinolytic protease (Clp) complex, which plays an essential role in maintaining protein homeostasis and comprises both plastid-encoded and nuclear-encoded subunits. They used plastome transformation to partially replace the native *clpP1* gene in tobacco with counterparts from different *Silene* species. The *Silene* variants differed in their amino acid sequence from the tobacco *clpP1* in a range from 5.1% to 63.0%. The results suggested that *Silene clpP1* with high divergence could not functionally replace the native copies of this gene. Other studies of this complex further indicated that the rates of *clpP1* evolution strongly correlate with the amino acid sequence divergence in interacting nuclear-encoded CLP counterparts in various angiosperms (Rockenbach et al., 2016; Williams et al., 2019). This may reflect the coevolution of genes involved in cytonuclear interactions to keep them functional (Abdel-Ghany et al., 2022; Ceriotti et al., 2022; Forsythe et al., 2021; Sloan et al., 2014; Williams et al., 2019). Among the genes involved in the cytonuclear complexes, we were able to identify *PSBW*, involved in the PSII supercomplex, with a biased expression in advanced generations, and differences in the amino acid sequence between *Lolium* and *Festuca*. These two aspects can potentially affect the entire complex including its overall functionality. A gradual increase of the *Lolium* variant over the *Festuca* in advanced generations may offer a clue about dynamics within the hybrid genome. This can be a result of cross-talk between specific transcription factors from each parent, post-transcriptional regulation, feedback regulation of protein synthesis, or other cellular features.

Another intriguing feature of the process is the involvement of the nuclear-encoded chaperonins and chaperones in the folding and assembly of the protein complexes encoded by nuclear and organelle genes. The most comprehensive overview was provided for RuBisCO (Li et al., 2022). In four different allopolyploids (wheat, cotton, tobacco, and Arabidopsis), chaperonins and chaperones of RuBisCO showed similar evolutionary genomic and transcriptomic patterns as the nuclear-encoded gene (*rbcS*): a frequent paternal-to-maternal homoeologous gene conversion and maternal HEB. These responses were temporally attenuated or even diminished during the folding and later assembly processes; chaperonins involved in

protein folding displayed more evidence of the cytonuclear coordination than chaperones functioning in later stages of protein assemblies. Not surprisingly, gene conversion of chaperonins and chaperones was frequently different in synthetically derived allopolyploids compared to their natural allopolyploid counterparts, with occasional examples of maternal-to-paternal conversion, whereas transcription trends were generally highly similar. In our hybrids of *F. pratensis* × *L. multiflorum*, we did not find any evidence of gene conversion, which is logical for the F_1 generation. However, the transcriptional regulation of chaperonin CPN60A was already predominantly biased towards the maternal parent at the HEB level, but only in one cross direction. ELD was biased towards *L. multiflorum* regardless of the direction of the cross (maternally in one cross direction). Considering the structural differences between *Lolium* and *Festuca* variants of *CPN60A* in highly conserved regions of the proteins, there may be another level of regulation within the hybrid genome that deals with the protein variant incompatibilities. Further studies are needed to uncover the regulatory mechanisms for overcoming cytonuclear hurdles that accompany hybridization and polyploidization in plants.

The multidisciplinary approach used in our study offers a unique overview of the mechanisms of the restoration of the stoichiometry of nuclear and organellar components involved in cytonuclear complexes after WGD and interspecific hybridization. Using newly established auto- and allopolyploids, we were able to monitor various biological processes instant after the whole-genome changes. This represents the most extensive investigation of the cytonuclear interactions in a single complex of auto- and allopolyploids. We found out that autopolyploids appear to compensate for the doubled nuclear ploidy with elevated organelle genome copy number, which exceeds the increase in the number of organelles (i.e. each chloroplast in polyploids has more circular DNA molecules than in diploids). The expression of both organelle-targeted nuclear and organellar genes is only meagerly modified. Our study of allopolyploids uncovered potential structural conflict in the parental protein variants involved in the cytonuclear complexes and suggests that maternal HEB and ELD are not involved in overcoming this issue. We are aware that our study does not provide the entire picture; post-trancriptional regulation, as a key regulatory process in the expression of organellar genes, needs to be explored in future research (Woodson & Chory, 2008), but this study provides a first step towards these experiments.

EXPERIMENTAL PROCEDURES

Plant material and growth conditions

The plant material consisted of five diploid ($2n = 2x = 14$) and five tetraploid ($2n = 4x = 28$) cultivars of *F. pratensis* Huds. and *L. multiflorum* Lam., a newly established autotetraploid of *F. pratensis* (C_0; $2n = 4x = 28$) that was developed by colchicine treatment of the ramets cloned from the individual plants and obtained from DLF Seeds plant breeding station (V. Černoch, Hladké Životice) and *Festuca* × *Lolium* homoploid ($2n = 2x = 14$; 7 *Lolium* + 7 *Festuca* chromosomes) and allotetraploid ($2n = 4x = 28$; 14 *Lolium* + 14 *Festuca* chromosomes) hybrid plants. Homoploid hybrids (F_1 generation) of *L. perenne* L. × *F. pratensis* were developed by Stephan Hartmann (Bavarian State Research Center for Agriculture). Allotetraploids (F_1 generations) were generated reciprocally between autotetraploid *L. multiflorum* cv 'Mitos' and autotetraploid *F. pratensis* cv 'Westa' ($2n = 4x = 28$) and were obtained from the Institute of Plant Genetics PAS (Poznań, Poland). The list of all plant materials used in this study and their ploidy level is shown in Table S4.

Seeds of all *F. pratensis* and *L. multiflorum* cultivars were germinated for 5 days on a wet filter paper at 25°C in the dark. Germinating kernels were planted in 10 × 10 cm pots filled with a mixture of soil and sand (3/1; v/v) and grown in a climatic chamber under controlled long-day conditions (16 h light with 200 μmol m^{-2} sec^{-1} light intensity and 22°C; 8 h dark at 16°C) with 60% humidity. F_1 hybrids were grown in 15 × 15 cm pots (filled with a mixture of soil and sand (3/1; v/v)) in the same climatic chamber.

Evaluation of morphological characters

Cell volume, chloroplast number and volume, and nucleus volume were examined on cryostat (Leica) generated sections. Leaves from five individuals of each genotype were collected, fixed in 4% paraformaldehyde and 1x phosphate-buffered saline (PBS; pH 7.0) for 2 h at room temperature (RT) and dehydrated in the sucrose gradient (33%, 50%, 66% and 100% of 2.3 M sucrose) for 1 h per step at RT. The samples in 2.3 M sucrose were kept overnight at 4°C and then used for cryostat sectioning. The tissue was embedded in Cryo-gel (Leica Microsystems, Richmond, IL, USA) and frozen at −25°C. A 20 μm thick sections were cut using Leica CM1950 cryostat, transferred to a microscope slide, stained with 4′,6-diamidino-2-phenylindole (DAPI) and stored in the dark at 4°C. Slides were imaged using a confocal microscope Leica TCS SP8 equipped with the Leica Application Suite X (LAS-X) v.3.5.5 software with the Leica Lightning module (Leica Microsystems). Image stacks were captured in sequential scans through the HC PLAPO CS2 100×/1.44 oil objective and hybrid detectors (HyD). The confocal pinhole was set to 1 AU. For each leaf, 30–40 optical sections in 200 nm steps were taken and composed into a 3D model. The image stacks were processed using IMARIS 9.6 software (Bitplane AG, Schlieren, Switzerland). IMARIS functions 'Surface' and 'Spot Detection' were used for the manual analysis of each cell. Nuclear volume was determined from the rendering of the primary intensity of DAPI staining while using the 'Surfaces' function. In this study, 50–60 cells, 20–30 chloroplasts, and 10–30 nuclei were analyzed in each plant. All data are summarized in Table S5. Two-sample, two-tailed t-test was used to compare the means between the groups and an effect size was tested by Cohen's D test. Data analysis was carried out using R studio 2022.07.2. and data were visualized in ggplot2.

Chloroplast genome copy number counting using droplet digital PCR (ddPCR)

Genomic DNA (gDNA) was extracted from the leaves using the NucleoSpin Plant II kit following the manufacturer's instructions. Subsequently, all samples were digested with 20 U of *Hin*dIII restriction enzyme for 4 h to improve ddPCR efficiency. Three

chloroplast-encoded genes involved in different cytonuclear complexes were selected to estimate the number of copies of the chloroplast genome in the samples: *ATPI*, *PSBD*, and *RBCL*. The chloroplast non-interacting gene *NDHB* was used as a control. A single-copy nuclear gene *ACT2* was analyzed as a proxy to calculate number of nuclei/cells in the sample (see below). Primers were designed to amplify approximately 100 bp region of each gene (Table S6). BLAST search of expected amplicons against the genome assembly was employed to avoid amplification from multiple genomic regions. Primer sequences were identical for both *L. multiflorum* and *F. pratensis* homoeologs. A 20 μl ddPCR reaction contained 10 μl BioRad QX200 ddPCR EvaGreen Supermix (BioRad, Hercules, CA, USA), 100 nM forward and reverse primer, and 0.1 ng gDNA for chloroplast genes or 10 ng gDNA for nuclear genes. Reducing amount of gDNA for chloroplast genes was necessary to avoid oversaturation with positive droplets. Samples were partitioned into droplets using DG8TM QX100TM/QX200TM Drop Generator Cartridges in BioRAD QX200™ Droplet Generator according to manufacturer's instructions and transferred into 96-well plate for PCR amplification. The plates were sealed using the BioRad PX1 PCR Plate Sealer. Amplification of the genes of interest was carried out as follows: 5 min at 95°C followed by 40 cycles of 30 sec at 95°C and 1 min at 59°C. Final signal stabilization was performed for 5 min at 4°C and 5 min at 90°C. The ramp rate was set to 2°C/sec per each change of temperature. Positive droplets were counted by Bio-Rad QX200 Droplet Reader and calculations of the copy number per sample were performed by Bio-Rad Quantasoft v1.7 software applying Poisson statistics. The nuclear gene copy number per sample was divided by the ploidy of the sample to estimate the number of nuclei /cells in the reaction. Subsequently, chloroplast gene copy number per sample was divided by the number of nuclei to calculate chloroplast gene copy number per cell. For *NDHB*, this result was divided by two to account for the fact that it is a two-copy gene. Statistical analyses were performed as described in the previous section. The experiment included four biological and two technical replicates and was repeated twice. The data are summarized in Table S7.

Gene expression analysis

Total RNA was isolated from leaves using the RNeasy Kit (Qiagen, Hilden, Germany), following the manufacturer's instructions. The quantity and quality of the RNA samples were measured using Qubit Fluorometric (Life Technologies, Eugene, OR, USA), Nanodrop ND-1000 spectrophotometer (Nanodrop Technologies, USA), and 1% agarose gel electrophoresis. To remove any remaining DNA, the RNA samples were treated with DNase I (Thermo Scientific™, Vilnius, Lithuania), before cDNA synthesis, which was performed using the RevertAid First Strand cDNA Synthesis Kit (Thermo Scientific™). For quantitative real-time PCR (qRT-PCR), a CFX96TM Real-Time PCR Detection System (Bio-Rad, USA) was used. Each experiment consisted of five biological and two technical replicates. The qRT-PCR cycling program consisted of an initial denaturation step at 94°C for 2 min, followed by 40 cycles of denaturation at 94°C for 15 sec, annealing at 58°C for 15 sec, and extension at 72°C for 20 sec. qRT-PCR was performed using qPCR 2X SYBR Master Mix (Top-Bio, Czech Republic). A melting curve analysis was conducted by ramping the temperature from 65 to 95°C to confirm the specificity of the amplified products. The $2^{-\Delta\Delta Cq}$ method (Livak & Schmittgen, 2001) was employed to analyze the transcript fold-changes using Maestro software v 2.0 (Bio–Rad, USA). The constitutively expressed gene *MATK* was chosen as the chloroplast reference gene, while the *ACT21* and *EIF4A* genes (Huang et al., 2014; Lechowicz et al., 2020) were selected as the reference genes for nuclear transcripts. The primer sequences used for qRT-PCR are provided in Table S6. The data are summarized in Table S8.

Chloroplast inheritance pattern

The DNeasy Kit (Qiagen) was used to extract gDNA from leaves of hybrids and their progenitors for chloroplast genotyping. Two chloroplast genes *ATPI* and *PSBD* were amplified using Q5® High-Fidelity DNA Polymerase from the gDNA. PCR products were sequenced via the Sanger method. The amplified fragments were analyzed to identify SNPs and consequently ascertain chloroplast inheritance patterns. The BigDye1 Terminator v3.1 Cycle Sequencing Kit (Applied Biosystems, Vilnius, Lithuania) was used for sequencing reactions, and the Agencourt Clean SEQ Dye-Terminator Removal Kit (Beckman Coulter, Brea, CA, USA) was used for purification. Sequences were determined using an ABI3730xl DNA analyzer. Sequence analysis was subsequently performed using Geneious Prime version 2023.1.1 (http://www.geneious.com).

Expression level dominance (ELD) and Homoeolog expression bias (HEB)

We performed analysis of ELD and HEB as previously described for the same set of plant materials (Glombik et al., 2021).

Relative allelic transcription of nuclear genes

Whole transcriptome data analysis was employed to determine the HEB of the genes involved in cytonuclear complexes. To confirm the RNA-seq results determining HEB (Glombik et al., 2021), cDNA samples from both homoploids and allopolyploids were analyzed using quantitative Sanger sequencing (qSanger) (Liu et al., 2022; Prakash et al., 2023). Specific primers were designed to target nuclear genes encompassing regions containing SNPs (Table S6) and the resulting PCR products were subsequently sequenced as previously described. All experiments were conducted in triplicate, addressing potential errors associated with sample preparation, PCR amplification, Sanger sequencing, and batch effects. The number of PCR cycles in the BigDye1 terminator reaction was reduced to 27 to maintain amplification within the exponential phase (Wilkening et al., 2005). Differences in peak heights corresponding to each SNP observed in the chromatograms were utilized to determine the proportions of each allele within the sample. For this purpose, the Quantitative Analysis of Sequence Variants (QSVanalyser) v 1.0.4 software was employed (Carr et al., 2009).

Mapping of substituted amino acids

Coding sequences of the genes of interest for both *Lolium* and *Festuca* variants were obtained from transcriptomes generated in our previous study (Glombik et al., 2021). To confirm the sequences, CDS sequences were amplified using Q5® High-Fidelity DNA Polymerase and subsequently subjected to Sanger sequencing, as previously described. The DNA sequences obtained from Sanger sequencing were translated into their respective amino acid sequences using Geneious Prime version 2023.1.1. The functional domains of each protein in the amino acid sequence were predicted using the Conserved Domain Database (CDD). The BLAST tool was utilized to analyze the protein sequences and identify highly conserved amino acids. A total of 20 similar sequences of the protein of interest were aligned and predicted. The relationship between the mutations and the functional domain was further characterized. The Alpha-fold web server was used to conduct structural modeling of proteins in order to examine the impact of SNPs on protein structure and

surface charge (Jumper et al., 2021). The models were visualized using PyMol v4.6.0 (Schrödinger, LLC). The surface electrostatic potential was analyzed using the APBS (v3.4.1) plugin, which is an Adaptive Poisson-Boltzmann Solver.

ACKNOWLEDGEMENTS

This research was funded by the Czech Science Foundation (grant awards 22-03731S). We would like to express our thanks to Prof. Adam J. Lukaszewski for their critical reading and valuable comments. Open access publishing facilitated by Ustav experimentalni botaniky Akademie ved Ceske republiky, as part of the Wiley - CzechELib agreement.

AUTHOR CONTRIBUTIONS

Conceptualization MSh, JM, MG, DKo, JK; Methodology MSh, JM, MG, DKo, JK; Formal analysis MSh, JM, DKu, MG, MSz, JK; Investigation MSh, JM, DKu, MG, MSz, JK; Resources ZZ, SH, DK; Data Curation MSh, MG, MSz; Writing—Original Draft MSh, DKo, JK; Writing—Review and Editing JM, ZZ, MG, JFW, JS, SH, MSz, JD, JB; Visualization MSh, JK; Supervision JFW, JS, JD, JB, DKo, JK; Project administration DKo, Funding acquisition DKo.

CONFLICT OF INTEREST

The authors declare no conflict of interest.

DATA AVAILABILITY STATEMENT

All relevant data can be found within the manuscript and its supporting materials.

SUPPORTING INFORMATION

Additional Supporting Information may be found in the online version of this article.

Figure S1. Chloroplast inheritance pattern. Characterization of chloroplast inheritance patterns through Sanger sequencing. *ATPI* (a) and *PSBD* (b) in homoploid (2*x*) and allotetraploid (4*x*) reciprocal hybrids of *Lolium* × *Festuca* and *Festuca* × *Lolium*.

Figure S2. Examples of quantitative Sanger sequencing results utilizing the QSV analyzer for allelic discrimination and quantification in the hybrids. Hybrid cDNA samples were used. (a) *ATPC1*, (b) *PPD7*, and (c) *PSBR*.

Table S1. Homoeolog expression bias analysis of cytonuclear genes and assembly factors in reciprocal hybrids.

Table S2. qSanger data.

Table S3. Amino acid differences between chloroplast genomes of *L. multiflorum, L. perenne, and F. pratensis*.

Table S4. Plant material.

Table S5. Cell analysis data: cell volume, nucleus volume, chloroplast volume measurements, and chloroplast counts.

Table S6. ddPCR, qPCR, and qSanger primers.

Table S7. ddPCR data.

Table S8. qPCR data.

REFERENCES

Abdel-Ghany, S.E., **LaManna, L.M.**, **Harroun, H.T.**, **Maliga, P.** & **Sloan, D.B.** (2022) Rapid sequence evolution is associated with genetic incompatibilities in the plastid Clp complex. *Plant Molecular Biology*, **108**, 277–287.

Bingham, E.T. (1968) Stomatal chloroplasts in alfalfa at 4x ploidy levels. *Crop Science*, **8**, 509–510.

Birky, C.W. (1995) Uniparental inheritance of mitochondrial and chloroplast genes – mechanisms and evolution. *Proceedings of the National Academy of Sciences of the United States of America*, **92**, 11331–11338.

Bomblies, K. (2020) When everything changes at once: finding a new normal after genome duplication. *Proceedings of the Royal Society B: Biological Sciences*, **287**, 20202154.

Butterfass, T. (1991) Cell sizes and chloroplast numbers per cell of Hemiploid and polyploid plants. *Cytologia*, **56**, 473–478.

Carr, I.M., **Robinson, J.I.**, **Dimitriou, R.**, **Markham, A.F.**, **Morgan, A.W.** & **Bonthron, D.T.** (2009) Inferring relative proportions of DNA variants from sequencing electropherograms. *Bioinformatics*, **25**, 3244–3250.

Ceriotti, L.F., **Gatica-Soria, L.** & **Sanchez-Puerta, M.V.** (2022) Cytonuclear coevolution in a holoparasitic plant with highly disparate organellar genomes. *Plant Molecular Biology*, **109**, 673–688.

Coate, J.E., **Schreyer, W.M.**, **Kum, D.** & **Doyle, J.J.** (2020) Robust cytonuclear coordination of transcription in nascent *Arabidopsis thaliana* autopolyploids. *Genes*, **11**, 134.

Ding, M.Q. & **Chen, Z.J.** (2018) Epigenetic perspectives on the evolution and domestication of polyploid plant and crops. *Current Opinion in Plant Biology*, **42**, 37–48.

Fernandes Gyorfy, M., **Miller, E.R.**, **Conover, J.L.**, **Grover, C.E.**, **Wendel, J.F.**, **Sloan, D.B.** ***et al.*** (2021) Nuclear-cytoplasmic balance: whole genome duplications induce elevated organellar genome copy number. *Plant Journal*, **108**, 219–230.

Ferreira de Carvalho, J., **Lucas, J.**, **Deniot, G.**, **Falentin, C.**, **Filangi, O.**, **Gilet, M.** ***et al.*** (2019) Cytonuclear interactions remain stable during allopolyploid evolution despite repeated whole-genome duplications in *Brassica*. *Plant Journal*, **98**, 434–447.

Forsythe, E.S., **Grover, C.E.**, **Miller, E.R.**, **Conover, J.L.**, **Arick, M.A.**, **Chavarro, M.C.F.** ***et al.*** (2022) Organellar transcripts dominate the cellular mRNA pool across plants of varying ploidy levels. *Proceedings of the National Academy of Sciences of the United States of America*, **119**, e2204187119.

Forsythe, E.S., **Williams, A.M.** & **Sloan, D.B.** (2021) Genome-wide signatures of plastid-nuclear coevolution point to repeated perturbations of plastid proteostasis systems across angiosperms. *Plant Cell*, **33**, 980–997.

Fox, D.T., **Soltis, D.E.**, **Soltis, P.S.**, **Ashman, T.L.** & **Van de Peer, Y.** (2020) Polyploidy: a biological force from cells to ecosystems. *Trends in Cell Biology*, **30**, 688–694.

Gasteiger, E., **Gattiker, A.**, **Hoogland, C.**, **Ivanyi, I.**, **Appel, R.D.** & **Bairoch, A.** (2003) ExPASy: the proteomics server for in-depth protein knowledge and analysis. *Nucleic Acids Research*, **31**, 3784–3788.

Germain, A., **Hotto, A.M.**, **Barkan, A.** & **Stern, D.B.** (2013) RNA processing and decay in plastids. *Wiley Interdisciplinary Reviews: RNA*, **4**, 295–316.

Glombik, M., **Bačovský, V.**, **Hobza, R.** & **Kopecký, D.** (2020) Competition of parental genomes in plant hybrids. *Frontiers in Plant Science*, **11**, 200.

Glombik, M., **Copetti, D.**, **Bartos, J.**, **Stoces, S.**, **Zwierzykowski, Z.**, **Ruttink, T.** ***et al.*** (2021) Reciprocal allopolyploid grasses (*festuca* × *Lolium*) display stable patterns of genome dominance. *Plant Journal*, **107**, 1166–1182.

Gong, L., **Olson, M.** & **Wendel, J.F.** (2014) Cytonuclear evolution of Rubisco in four allopolyploid lineages. *Molecular Biology and Evolution*, **31**, 2624–2636.

Gong, L., **Salmon, A.**, **Yoo, M.J.**, **Grupp, K.K.**, **Wang, Z.N.**, **Paterson, A.H.** ***et al.*** (2012) The cytonuclear dimension of allopolyploid evolution: an example from cotton using rubisco. *Molecular Biology and Evolution*, **29**, 3023–3036.

Greiner, S., **Sobanski, J.** & **Bock, R.** (2015) Why are most organelle genomes transmitted maternally? *BioEssays*, **37**, 80–94.

Grover, C.E., **Forsythe, E.S.**, **Sharbrough, J.**, **Miller, E.R.**, **Conover, J.L.**, **DeTar, R.A.** ***et al.*** (2022) Variation in cytonuclear expression accommodation among allopolyploid plants. *Genetics*, **222**, iyac118.

Grover, C.E., **Gallagher, J.P.**, **Szadkowski, E.P.**, **Yoo, M.J.**, **Flagel, L.E.** & **Wendel, J.F.** (2012) Homoeolog expression bias and expression level dominance in allopolyploids. *New Phytologist*, **196**, 966–971.

Huang, L.K., **Yan, H.D.**, **Jiang, X.M.**, **Yin, G.H.**, **Zhang, X.Q.**, **Qi, X.** ***et al.*** (2014) Identification of candidate reference genes in perennial ryegrass for quantitative RT-PCR under various abiotic stress conditions. *PLoS One*, **9**, e93724.

Jarvis, D.E., **Ho, Y.S.**, **Lightfoot, D.J.**, **Schmöckel, S.M.**, **Li, B.**, **Borm, T.J.A.** ***et al.*** (2017) The genome of *Chenopodium quinoa*. *Nature*, **542**, 307–312.

Jiao, Y.N., **Wickett, N.J.**, **Ayyampalayam, S.**, **Chanderbali, A.S.**, **Landherr, L.**, **Ralph, P.E.** ***et al.*** (2011) Ancestral polyploidy in seed plants and angiosperms. *Nature*, **473**, 97–100.

Jumper, J., **Evans, R.**, **Pritzel, A.**, **Green, T.**, **Figurnov, M.**, **Ronneberger, O.** ***et al.*** (2021) Highly accurate protein structure prediction with AlphaFold. *Nature*, **596**, 583–589.

Kawade, K., **Horiguchi, G.**, **Ishikawa, N.**, **Hirai, M.Y.** & **Tsukaya, H.** (2013) Promotion of chloroplast proliferation upon enhanced post-mitotic cell expansion in leaves. *BMC Plant Biology*, **13**, 143.

Kiang, A.S., **Connolly, V.**, **McConnell, D.J.** & **Kavanagh, T.A.** (1994) Paternal inheritance of mitochondria and chloroplasts in *Festuca pratensis* – *Lolium perenne* intergeneric hybrids. *Theoretical and Applied Genetics*, **87**, 681–688.

Kopecky, D., **Bartos, J.**, **Zwierzykowski, Z.** & **Dolezel, J.** (2009) Chromosome pairing of individual genomes in tall fescue (Festuca arundinacea Schreb.), its progenitors, and hybrids with Italian ryegrass (Lolium multiflorum lam.). *Cytogenetic and Genome Research*, **124**, 170–178.

Lechowicz, K., **Pawlowicz, I.**, **Perlikowski, D.**, **Arasimowicz-Jelonek, M.**, **Majka, J.**, **Augustyniak, A.** ***et al.*** (2020) Two *festuca* species - *F. Arundinacea* and *F. Glaucescens* - differ in the molecular response to drought, while their physiological response is similar. *International Journal of Molecular Sciences*, **21**, 3174.

Li, C.P., **Ding, B.X.**, **Ma, X.T.**, **Yang, X.**, **Wang, H.Y.**, **Dong, Y.F.** ***et al.*** (2022) A temporal gradient of cytonuclear coordination of chaperonins and chaperones during RuBisCo biogenesis in allopolyploid plants. *Proceedings of the National Academy of Sciences of the United States of America*, **119**, e2200106119.

Li, C.P., **Sun, X.H.**, **Conover, J.L.**, **Zhang, Z.B.**, **Wang, J.B.**, **Wang, X.F.** ***et al.*** (2019) Cytonuclear coevolution following homoploid hybrid speciation in *Aegilops tauschii*. *Molecular Biology and Evolution*, **36**, 341–349.

Li, C.P., **Wang, X.F.**, **Xiao, Y.X.**, **Sun, X.H.**, **Wang, J.B.**, **Yang, X.** ***et al.*** (2020) Coevolution in hybrid genomes: nuclear-encoded rubisco small subunits and their plastid-targeting Translocons accompanying sequential allopolyploidy events in *Triticum*. *Molecular Biology and Evolution*, **37**, 3409–3422.

Liu, Y., **Liu, J.Y.**, **Plante, K.S.**, **Plante, J.A.**, **Xie, X.P.**, **Zhang, X.W.** ***et al.*** (2022) The N501Y spike substitution enhances SARS-CoV-2 infection and transmission. *Nature*, **602**, 294–299.

Livak, K.J. & **Schmittgen, T.D.** (2001) Analysis of relative gene expression data using real-time quantitative PCR and the 2(T)(-Delta Delta C) method. *Methods*, **25**, 402–408.

Majka, J., **Glombik, M.**, **Dolezalová, A.**, **Knerová, J.**, **Ferreira, M.T.M.**, **Zwierzykowski, Z.** ***et al.*** (2023) Both male and female meiosis contribute to non-mendelian inheritance of parental chromosomes in interspecific plant hybrids *Lolium* x *festuca*. *New Phytologist*, **238**, 624–636.

Mochizuki, A. & **Sueoka, N.** (1955) Genetic studies on the number of plastid in stomata I. Effects of autopolyploidy in sugar beets. *Cytologia*, **20**, 358–366.

Oberprieler, C., **Talianova, M.** & **Griesenbec, J.** (2019) Effects of polyploidy on the coordination of gene expression between organellar and nuclear genomes in *leucanthemum* mill. (Compositae, Anthemideae). *Ecology and Evolution*, **9**, 9100–9110.

Prakash, S., **Racovita, A.**, **Petrucci, T.**, **Galizi, R.** & **Jaramillo, A.** (2023) qSanger: quantification of genetic variants in bacterial cultures by sanger sequencing. *Biodesign Research*, **5**, 0007.

Pyke, K.A. & **Leech, R.M.** (1987) The control of chloroplast number in wheat mesophyll-cells. *Planta*, **170**, 416–420.

Rand, D.M., **Haney, R.A.** & **Fry, A.J.** (2004) Cytonuclear coevolution: the genomics of cooperation. *Trends in Ecology & Evolution*, **19**, 645–653.

Rapp, R.A., **Udall, J.A.** & **Wendel, J.F.** (2009) Genomic expression dominance in allopolyploids. *BMC Biology*, **7**, 18.

Renny-Byfield, S. & **Wendel, J.F.** (2014) Doubling down on genomes: polyploidy and crop plants. *American Journal of Botany*, **101**, 1711–1725.

Rockenbach, K., **Havird, J.C.**, **Monroe, J.G.**, **Triant, D.A.**, **Taylor, D.R.** & **Sloan, D.B.** (2016) Positive selection in rapidly evolving plastid-nuclear enzyme complexes. *Genetics*, **204**, 1507–1522.

Roux, F., **Mary-Huard, T.**, **Barillot, E.**, **Wenes, E.**, **Botran, L.**, **Durand, S.** ***et al.*** (2016) Cytonuclear interactions affect adaptive traits of the annual plant *Arabidopsis thaliana* in the field. *Proceedings of the National Academy of Sciences of the United States of America*, **113**, 3687–3692.

Salman-Minkov, A., **Sabath, N.** & **Mayrose, I.** (2016) Whole-genome duplication as a key factor in crop domestication. *Nature Plants*, **2**, 16115.

Sehrish, T., **Symonds, V.V.**, **Soltis, D.E.**, **Soltis, P.S.** & **Tate, J.A.** (2015) Cytonuclear coordination is not immediate upon allopolyploid formation in *Tragopogon miscellus* (Asteraceae) allopolyploids. *PLoS One*, **10**, e0144339.

Shan, S.C., **Boatwright, J.L.**, **Liu, X.X.**, **Chanderbali, A.S.**, **Fu, C.N.**, **Soltis, P.S.** ***et al.*** (2020) Transcriptome dynamics of the inflorescence in reciprocally formed allopolyploid *Tragopogon miscellus* (Asteraceae). *Frontiers in Genetics*, **11**, 888.

Sharbrough, J., **Conover, J.L.**, **Fernandes Gyorfy, M.**, **Grover, C.E.**, **Miller, E.R.**, **Wendel, J.F.** ***et al.*** (2022) Global patterns of subgenome evolution in organelle-targeted genes of six allotetraploid angiosperms. *Molecular Biology and Evolution*, **39**, msac074.

Sharbrough, J., **Conover, J.L.**, **Tate, J.A.**, **Wendel, J.F.** & **Sloan, D.B.** (2017) Cytonuclear responses to genome doubling. *American Journal of Botany*, **104**, 1277–1280.

Sloan, D.B., **Triant, D.A.**, **Forrester, N.J.**, **Bergner, L.M.**, **Wu, M.** & **Taylor, D.R.** (2014) A recurring syndrome of accelerated plastid genome evolution in the angiosperm tribe Sileneae (Caryophyllaceae). *Molecular Phylogenetics and Evolution*, **72**, 82–89.

Soltis, P.S. & **Soltis, D.E.** (2009) The role of hybridization in plant speciation. *Annual Review of Plant Biology*, **60**, 561–588.

Soltis, P.S. & **Soltis, D.E.** (2016) Ancient WGD events as drivers of key innovations in angiosperms. *Current Opinion in Plant Biology*, **30**, 159–165.

Song, Q.X. & **Chen, Z.J.** (2015) Epigenetic and developmental regulation in plant polyploids. *Current Opinion in Plant Biology*, **24**, 101–109.

Svačina, R., **Sourdille, P.**, **Kopecký, D.** & **Bartoš, J.** (2020) Chromosome pairing in polyploid grasses. *Frontiers in Plant Science*, **11**, 1056.

Van de Peer, Y., **Ashman, T.L.**, **Soltis, P.S.** & **Soltis, D.E.** (2021) Polyploidy: an evolutionary and ecological force in stressful times. *Plant Cell*, **33**, 11–26.

Van de Peer, Y., **Mizrachi, E.** & **Marchal, K.** (2017) The evolutionary significance of polyploidy. *Nature Reviews Genetics*, **18**, 411–424.

Wang, X.F., **Dong, Q.L.**, **Li, X.C.**, **Yuliang, A.Z.**, **Yu, Y.N.**, **Li, N.** ***et al.*** (2017) Cytonuclear variation of rubisco in synthesized rice hybrids and allotetraploids. *Plant Genome*, **10**.

Wendel, J.F. (2015) The wondrous cycles of polyploidy in plants. *American Journal of Botany*, **102**, 1753–1756.

Wilkening, S., **Hemminki, K.**, **Thirumaran, R.K.**, **Bermejo, J.L.**, **Bonn, S.**, **Forsti, A.** ***et al.*** (2005) Determination of allele frequency in pooled DNA: comparison of three PCR-based methods. *BioTechniques*, **39**, 853–858.

Williams, A.M., **Friso, G.**, **van Wijk, K.J.** & **Sloan, D.B.** (2019) Extreme variation in rates of evolution in the plastid Clp protease complex. *Plant Journal*, **98**, 243–259.

Woodson, J.D. & **Chory, J.** (2008) Coordination of gene expression between organellar and nuclear genomes. *Nature Reviews Genetics*, **9**, 383–395.

Xia, L.Y., **Jiang, Y.L.**, **Kong, W.W.**, **Sun, H.**, **Li, W.F.**, **Chen, Y.X.** ***et al.*** (2020) Molecular basis for the assembly of RuBisCO assisted by the chaperone Raf1. *Nature Plants*, **6**, 708–717.

Yoo, M.J., **Liu, X.X.**, **Pires, J.C.**, **Soltis, P.S.** & **Soltis, D.E.** (2014) Nonadditive gene expression in polyploids. *Annual Review of Genetics*, **48**, 485–517.

Zhai, Y.F., **Yu, X.Q.**, **Zhu, Z.B.**, **Wang, P.Q.**, **Meng, Y.**, **Zhao, Q.Z.** ***et al.*** (2019) Nuclear-cytoplasmic coevolution analysis of RuBisCO in synthesized *Cucumis* allopolyploid. *Genes*, **10**, 869.